THE ASTROPHYSICAL JOURNAL, 373:482–496, 1991 June 1

C AND N ABUNDANCES AMONG 47 TUCANAE MAIN-SEQUENCE STARS

MICHAEL M. BRILEY[1,2]
McDonald Observatory, University of Texas at Austin, Austin, TX 78712

JAMES E. HESSER[1]
Dominion Astrophysical Observatory, Herzberg Institute of Astrophysics, National Research Council,
5071 West Saanich Road, Victoria, BC, Canada V8X 4M6

AND

R. A. BELL
Astronomy Program, University of Maryland, College Park, MD 20742

Received 1990 June 15; accepted 1990 November 26

ABSTRACT

The CTIO 4 m telescope, RC spectrograph, and the "2D-FRUTTI" detector have been used to obtain spectra for 20 47 Tuc (=NGC 104 = C0021−723) stars. The stars observed were 10 main-sequence (MS), four luminous red-giants, and six subgiants, giving a total observed range of $12.1 < V < 18.5$ ($-1.2 < M_V < 5.2$). Variations in CN and CH band strengths were detected across the entire range. The CN and CH band strengths have been analyzed using the $S(3839)$ and s_{CH} spectral indices, which have been compared to indices from corresponding synthetic spectra to obtain abundances. An Mg-sensitive index, Mg_2, has also been measured, with the result that there is no observed correlation between Mg_2 and CN-band strength.

The observed C and N abundance variations are impossible to reproduce with the assumptions of mixing involving only C → N-processed material and initial C and N abundances appropriate to either the CN-normal stars or the solar ratio. Adding the possibility of O → N-cycle mixing will allow total C + N + O to be conserved. However, abandoning the assumption of CNO in the solar ratio will allow CN-process mixing to result in the observed C and N abundances while maintaining constant C + N, but mixing of the CN-normal stars is then also required.

The distribution of CN band strengths appears to be consistent with the existence on the upper MS of the 3883 Å CN bimodality, previously observed throughout the more evolved regions of the CM-diagram. Any mixing episode(s) hypothesized to account for the CN and CH variations must therefore have taken place before the upper MS. The C and N abundance differences are very similar to the differences observed among the more luminous cluster stars. Any discussion of mechanisms for altering the surface C, N, and O abundances (as well as isotopic ratios) of evolved stars must allow for a significant population of upper MS stars with strong CN bands, which would appear to represent a greater challenge at present for mixing, rather than for primordial, mechanisms.

Subject headings: clusters: globular — stars: abundances

1. INTRODUCTION

The nearby Galactic globular cluster 47 Tucanae has long been known to be inhomogeneous in the C and N abundances of its member stars. These star to star differences have been traced by various investigators from the red giant branch (RGB) tip to the asymptotic giant branch (AGB) and horizontal branch (HB), to the subgiant branch (SGB), and even down to the MS turnoff (Bell, Dickens, & Gustafsson 1975; Hesser, Hartwick, & McClure 1976, 1977; Hesser 1978; Mallia 1978; Norris 1978; Norris & Freeman 1979; Norris & Cottrell 1979; Dickens, Bell, & Gustafsson 1979; Hesser & Bell 1980; Bell, Hesser, & Cannon 1983; Norris, Freeman, & DaCosta 1984; Smith, Bell, & Hesser 1989 (hereafter SBH); and Briley et al. 1989 [hereafter BBSH]). The distribution of 3883 Å CN band strengths on the HB (Norris & Freeman 1982), AGB, RGB (Norris 1978; Norris & Freeman 1979), and SGB (BBSH) is noticeably bimodal, and is accompanied by an anticorrelation between CN and CH band strengths. The bimodal distributions have been suggested to be the result of saturation in the strengths of the 3883 or 4215 Å CN bands (Suntzeff 1981; Langer 1985; BBSH). Other variations, including a correlation between Na atomic lines and CN have also been observed (Cottrell & Da Costa 1981; Lloyd Evans, Menzies, & Smith 1982). Similar abundance trends are also known to occur in a large number of other metal-rich to moderate ($-0.8 <$ [Fe/H] < -1.6) globular clusters (see Smith 1987 and Suntzeff 1988 for reviews). Yet, despite the apparently common occurrence of these variations, and the tremendous research effort which has been made in their study, the origins of the variations remain uncertain.

Two possibilities have been put forth as explanations of the C and N abundance differences in general. The first is that the variations are the result of a process or processes within the stars themselves that chemically alter the material and bring it to the surface by a mixing or diffusion mechanism (such as the circulation of envelope material through the C → N-cycle region). The second hypothesis is that the low-mass cluster stars formed from material which was originally inhomogeneous in C and N (a primordial origin). Arguments may be made for and against each senario; see Smith (1987) and Sun-

[1] Visiting Astronomer, Cerro Tololo Inter-American Observatory, National Optical Astronomy Observatories, operated by AURA, Inc., under contract with the National Science Foundation.

[2] From a thesis submitted to the Graduate School, University of Maryland, in partial fulfillment of the requirements for the doctoral degree in astronomy.

tzeff (1988) for a comprehensive discussion. Other possible mechanisms include accretion, which can explain the overabundances of CN in stars near the turnoff, where the convection zone near the surface is thin and only a modest amount of material is needed to alter the surface composition. This is, however, unlikely for the giant stars, where the convective zone involves a much greater portion of the stars' mass. Somewhat more exotic processes, such as gravitational settling and turbulent diffusion (Genova & Schatzman 1979; Proffitt & Michaud 1990), have also been considered.

The earlier works of Hesser (1978), Hesser & Bell (1980), and Bell, Hesser, & Cannon (1983) observed spectroscopically 17 47 Tuc dwarfs (in total) at resolutions from 18 to 4 Å using the CTIO SIT vidicon. Their conclusions were that CN variations existed on the upper main sequence, at least down to $V \approx 17.6$ ($M_v \approx 4.3$). Given the improvements in detector systems since these earlier MS works, a new observational study seemed worthwhile, to characterize more accurately the nature of the CN-band strength variations among upper MS stars in 47 Tuc. The results from the MS stars will receive the most attention, as properties of the brighter stars have been fully discussed in previous papers (see SBH and BBSH).

2. OBSERVATIONS

Observations of 47 Tuc stars were taken on the nights of 1989 October 3/4–6/7 with the CTIO 4 m telescope and RC spectrograph with the 2D-FRUTTI. The KPGL No. 1 grating (632 lines mm^{-1} blazed at 4200 Å) was used at a tilt of 58°0. With a 200 μm slit (1″5) and the detector in 2 × 2 mode, each pixel corresponded to 1.47 Å, with a FWHM of 2.7 pixels, or 4.0 Å. The wavelength region covered was 3500–5500 Å. Integration times were generally 3600 s per exposure for the fainter stars (giving ~100 counts per pixel above the sky in the continuum redward of the 3883 Å CN region). Seeing ranged from ~1″5 to 3″, and there were some clouds on the second and third nights. The spectrograph was usually rotated to allow two program stars to fall simultaneously on the slit (ideally one CN-strong, one CN-normal; see below). Comparison spectra from an HeAr lamp were taken between each observation, with a long (1000 s) exposure at the start of each night to aide in the wavelength calibrations. Hour-long flat-field frames were also taken at the start of each night, with the grating at two different angles in order to obtain sufficient counts at both the red and blue ends of the spectra. Dark exposures (of order 10,000 s) were made after the second and third nights. Exposures of a multihole decker, illuminated by an incandescent lamp, were also made at the start of each night for use in the removal of the image tube's S-distortion. A number of flux standards were observed at the start and finish of each night.

The data were reduced at La Serena and College Park using IRAF (V2.8) on Sun workstations. The detailed steps in the reductions are the same as those outlined in SBH. As the number of photons detected from the faintest stars was comparable to or slightly less than those from the sky alone, great care was taken in avoiding background stars when selecting apertures for the sky subtraction. Identical apertures were used for each star in the slit (in the cases of multiple stars in a single observation) and for fields observed more than once. The reduced spectra from multiple observations of the same star were added together to increase the signal-to-noise ratio of the final spectrum.

Bell, Cannon, & Hesser obtained AAT Fiber Spectrograph data for a large sample of dwarf stars. These data have not been published yet, primarily owing to difficulties with the calibrations. However, the fainter stars observed for the present paper were largely chosen on their apparent 3883 Å CN strengths in the AAT data. An effort was made to select pairs of stars close enough together to be observed simultaneously and exhibiting 3883 Å band strength differences in the AAT data. The set of stars observed at CTIO is therefore not a random sample, but was chosen to allow more accurate band strength measurements in stars thought to show large differences in such strengths. A list of program stars is given in Table 1. Star designations and photometry were taken from Hesser & Hartwick (1977), Hesser et al. (1987), Lee (1977), or Walker (1989, private communication; see SBH). The observed portion of the CMD is shown in Figure 1, where V, $(B-V)$ values have been converted to M_V, $(B-V)_0$ using $E(B-V) = 0.04$ (Lee 1977) and an observed distance modulus of 13.40 (Hesser et al. 1987).

One curiosity is star H-20034, seen in Figure 1 to be slightly too red for its $M_V \approx +4.4$ brightness. If it were a background SMC star, it would then be a supergiant with an obviously different spectrum from that which was observed. Neither does it appear to be a foreground field star, as its A(Ca) index (a measure of Ca II absorption in the H + K line region; see Norris & Freeman 1982) is no different than the other 47 Tuc MS stars (as computed from the spectra before slope correc-

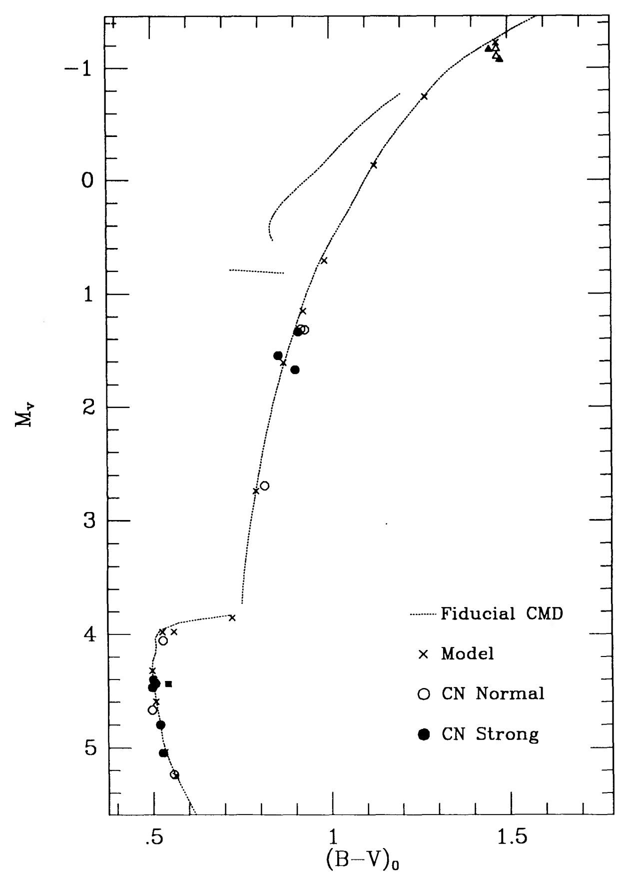

FIG. 1.—The fiducial H-R diagram for 47 Tuc of Hesser et al. (1987) (*dotted line*) has been plotted with the locations of the observed stars marked with circles, (SGB and MS stars), triangles (RGB stars), and a square (star H-20034; see § 2). Open markers indicate stars that were found to be CN-normal, while filled markers are the CN-strong stars. The colors of the models used in generating synthetic spectra (*crosses*) are also indicated.

TABLE 1

Observational Data for the Program Stars

Object[a]	V	M_V	$(B-V)_0$	$S(3839)(\sigma)$	$s_{CH}(\sigma)$	$\delta S(3839)$	δs_{CH}	$Mg_2(\sigma)$	Number of Observations	Time (s)	Pair Number	Night
HH-2077 (L-4418)	12.10	−1.17	1.47	0.264	0.279	...	...	0.281	1	600	...	3
HH-2006 (L-3501)	12.11	−1.16	1.45	0.412(0.094)	0.281(0.024)	...	...	0.285(0.005)	2	900	...	3
HH-3205 (L-5309)	12.17	−1.10	1.47	0.362	0.282	...	...	0.293	1	600	...	3
HH-3027 (L-5312)	12.20	−1.07	1.48	0.432	0.259	...	...	0.295	1	600	...	3
AW-1	14.585	1.32	0.918	0.299	0.289	...	...	0.117	1	600	...	2
AW-2	14.590	1.32	0.928	0.339(0.041)	0.289(0.030)	...	...	0.136(0.006)	2	1170	1	4
HH-9038	14.61	1.34	0.91	0.623(0.048)	0.289(0.008)	...	...	0.153(0.013)	4	1800	...	1, 2, 3, 4
AW-3	14.817	1.55	0.854	0.652	0.237	...	...	0.114	1	570	1	4
AW-4	14.944	1.67	0.902	0.450	0.290	...	...	0.157	1	600	...	2
AW-7	15.967	2.70	0.815	0.274	0.251	...	...	0.096	1	600	1	4
H-10014	17.328	4.06	0.529	−0.080(0.012)	0.191(0.036)	0.008	0.029	0.068(0.013)	2	7200	2	4
H-20030	17.673	4.40	0.502	0.078(0.024)	0.124(0.031)	0.177	−0.024	0.044(0.018)	3	10189	3	2
H-20032	17.706	4.44	0.508	0.083(0.028)	0.137(0.027)	0.180	0.030	0.062(0.010)	3	10800	4	1, 3
H-20033	17.707	4.44	0.505	−0.109(0.025)	0.156(0.009)	−0.012	0.006	0.084(0.009)	3	10189	3	2
H-20034	17.712	4.44	0.543	0.041(0.031)	0.167(0.006)	0.138	0.017	0.113(0.007)	3	12000	5	3
H-10023	17.743	4.47	0.499	0.006(0.086)	0.159(0.007)	0.102	0.008	0.078(0.001)	2	7200	2	4
H-20045	17.941	4.67	0.498	−0.148(0.035)	0.137(0.034)	−0.060	−0.023	0.070(0.011)	3	10800	4	1, 3
H-20053	18.070	4.80	0.521	0.064(0.031)	0.079(0.010)	0.148	−0.087	0.097(0.023)	3	12000	5	3
H-20068	18.316	5.05	0.528	0.069(0.030)	0.159(0.012)	0.136	−0.023	0.084(0.012)	5	18000	6	4
H-20083	18.509	5.24	0.558	−0.016(0.061)	0.210(0.009)	0.024	0.004	0.093(0.016)	5	18000	6	4

[a] Key to object codes.—AW, Walker (see SBH89); H, Hesser et al. 1987; HH, Hesser & Hartwick 1977; L, Lee 1977.

tions; see below). The difference in radial velocity (v_r) between H-20034 and the cluster mean, as computed from the present observations, is 24 km s^{-1}. However, the error in the observations are greater than this, as they yield a v_r of -27 ± 32 km s^{-1} (32 km $s^{-1} \approx 0.3$ pixel widths) for 47 Tuc. Mayor et al. (1984); Hesser, Shawl, & Meyer (1986) derived -19 ± 1 km s^{-1}. H-20034 may be an equal mass binary system within 47 Tuc (although the 47 Tuc CM-diagram suggests such stars are rare; see Hesser et al. 1987). As no convincing argument can be made for the star's exclusion from the data set, it will be included in the following analysis; however, the results derived from it should be viewed with caution.

3. ANALYSIS

A grid of plane-parallel, flux-constant, line-blanketed model atmospheres was calculated using the MARCS program (Gustafsson et al. 1975). The temperatures and gravities for these models were chosen such that their spectra, as computed from the SSG program (Bell & Gustafsson 1978), yielded the appropriate M_V and $(B-V)$ colors for points on the fiducial 47 Tuc CM-diagram of Hesser et al. (1987). The exact procedure for developing the grid is outlined in detail in Briley et al. (1990). An overall metallicity for 47 Tuc of [A/H] = -0.8 was assumed, as in SBH. A microturbulent velocity (ξ) of 2.0 km s^{-1} was used in the equation for total Doppler broadening velocity (DBV) of

$$\mathrm{DBV} = \sqrt{2kT/m + \xi^2} .$$

The effects of varying ξ are considered below (and found to be small). The masses used in the calculation of M_V were 0.85 $M_\odot$ for the MS, and 0.90 $M_\odot$ for the more evolved stars (following the isochrone fits of Hesser et al. 1987). The temperatures and gravities of the grid points are given in Table 2 and the resulting colors are plotted in Figure 1.

Synthetic spectra were then computed with a variety of C, N, and O abundances for each model in the grid (the logarithmic solar abundances of C, N, and O were taken to be 8.62, 8.00, and 8.86, respectively, on a scale of H = 12.0—these are taken, by default, as the reference values for 47 Tuc). The spectra covered 3500–5500 Å, with fluxes calculated at every 0.02 Å, and were smoothed by a Gaussian of appropriate width to match the 4.0 Å resolution of the observations. The values of C, N, and O used in the synthetic spectra followed the groups of SBH and BBSH. Thus group (A) has solar C, N, and O abundances, group (B) represents C → N-process material mixing (C + N held constant; [C/A] = -0.10, -0.30 and [N/A] = $+0.29$, $+0.49$, respectively), (C) represents C → N and O → N-process material mixing (in an arbitrary ratio with C + N + O held constant; [C/A] = -0.20, -0.30 and [N/A] = $+0.61$, $+0.76$ with [O/A] = -0.10 and -0.20, respectively), and group (D) stars have only a N excess ([C/A] = [O/A] = 0.00). Note that the group (B) [C/A] = -0.3, [N/A] = $+0.49$ synthetic spectra show the strongest CN bands among stars with $T_{\mathrm{eff}} > 4750$ K that can be obtained through C → N-process material mixing alone (holding C + N constant). Further mixings will deplete C, causing weaker CN bands, despite the greater N enhancements (Smith & Bell 1986). Initially, the $^{12}C/^{13}C$ ratio used was the solar value of 89. However, in light of recent work on ^{13}C in 47 Tuc (BBSH; Brown & Wallerstein 1989; Bell, Briley, & Smith 1990) which seems to indicate low $^{12}C/^{13}C$ ratios, at least on the upper giant branch and SGB of 47 Tuc, other spectra were computed with $^{12}C/^{13}C = 4$, as described below. The effects of different O abundances on the MS spectra were also investigated.

Comparisons between observed and synthetic spectra from stars of the same $(B-V)$ color showed small differences in overall continua slopes. It is believed these differences arise largely from differential refraction as the slit size was usually smaller than the stellar image. The effect causes zero point shifts in the measured indices, especially the single-sideband index $S(3839)$. A procedure was devised to correct for this, assuming the continua in the synthetic spectra to be more reliable than those in the observations. The fluxes in the regions given in Table 3 were summed for both observed and synthetic template spectra. Areas of strong CN, CH, and MgH absorption were avoided and synthetic spectra from the model grid with solar C, N, and O were used as the templates. A set of correction factors (equal to the sum over each region from Table 3 in the observed spectrum divided by the similar sum from the template) was computed. An interpolation in $(B-V)$ between the two synthetic template spectra closest in $(B-V)$ color was used to find the factors for observed stars between model points. A continuous correction function was then generated by running a cubic spline through the individual correction factors for each wavelength interval. The correction function was then smoothed by a 200 Å FWHM Gaussian to eliminate any ringing or short-wavelength fluctuations in the spline. The final step in the process was to multiply the observed spectrum by the correction function. An uncorrected and corrected spectrum for a typical star (H-20033) is shown in Figure 2, as well as the correction function which was employed. The identical process was also applied to all synthetic spectra of groups (B), (C), and (D), where the changes is slope were very small.

The $S(3829)$ index, a measure of CN absorption in the 3883 Å band, was determined in the same manner for both the observed and synthetic spectra. The index is defined as

$$S(3839) = -2.5 \log (F_{\lambda,\mathrm{FCN}}/F_{\lambda,\mathrm{CCN}}) .$$

A second index, s_{CH}, which quantifies the strength of the G band and is given by

$$s_{\mathrm{CH}} = -2.5 \log [2F_{\lambda,\mathrm{FCH}}/(F_{\lambda,\mathrm{CCH1}} + F_{\lambda,\mathrm{CCH2}})] ,$$

was also computed from the spectra, as well as the MgH and Mg b sensitive Mg_2 index from Faber et al. (1985), defined as

$$Mg_2 = -2.5 \log [F_{\lambda,\mathrm{FMG}}/(2F_{\lambda,\mathrm{CMG1}} + F_{\lambda,\mathrm{CMG2}})] .$$

In the above relations, F_λ refers to the mean flux per pixel over the specified wavelength range given in Table 4. The results of the index measurements are given in Tables 1 and 2. The errors quoted in Table 1 (in parentheses following indices) were determined from index measurements of the individual spectra from multiply observed stars, while the indices themselves were computed from the summed spectra.

Variations in $^{12}C/^{13}C$ will have a measurable effect on the strong 3883 Å bands of the RGB and SGB stars (Briley et al. 1989), but not on the weaker CN bands of the MS stars. This can be seen from a comparison of the indices computed from spectra with $^{12}C/^{13}C = 4$ in Table 2 as well as Figure 3. For the cooler stars, the added line blocking from a change in $^{12}C/^{13}C$ from 89 to 4 will result in changes in $S(3839)$ of ≥ 0.1 mag. For the MS stars, however, the change will be more of the order of 0.02 mag or less for both the CN strong and weak stars (see Table 2). The G-band strengths are far less sensitive

TABLE 2

A. Indices Derived from Synthetic Spectra

T_{eff}	logg	V	M_V	$(B-V)_0$	[C/A]	[N/A]	[O/A]	S(3839)	s_{CH}
Group A									
3825	0.90	12.05	-1.23	1.469	...	...	...	0.469	0.249
4050	1.30	12.53	-0.74	1.269	...	...	...	0.565	0.271
4250	1.70	13.14	-0.13	1.126	...	...	...	0.619	0.308
4500	2.20	13.98	0.71	0.985	...	...	...	0.570	0.325
4625	2.45	14.43	1.16	0.924	...	...	...	0.526	0.327
4750	2.70	14.88	1.61	0.869	...	...	...	0.466	0.325
4950	3.25	16.01	2.74	0.790	...	...	...	0.345	0.314
5150	3.76	17.13	3.86	0.722	...	...	...	0.226	0.298
5700	4.00	17.25	3.98	0.560	...	...	...	-0.047	0.203
5820	4.07	17.25	3.98	0.528	...	...	...	-0.079	0.174
5950	4.25	17.60	4.33	0.499	...	...	...	-0.100	0.147
5925	4.35	17.87	4.60	0.508	...	...	...	-0.091	0.157
5850	4.50	18.31	5.04	0.533	...	...	...	-0.068	0.181
5750	4.55	18.52	5.25	0.562	...	...	...	-0.038	0.208
Group B									
3825	0.90	12.05	-1.23	1.469	-0.10	+0.29	...	0.475	0.229
4050	1.30	12.53	-0.74	1.269	-0.10	+0.29	...	0.584	0.256
4250	1.70	13.14	-0.13	1.126	-0.10	+0.29	...	0.656	0.292
4500	2.20	13.98	0.71	0.985	-0.10	+0.29	...	0.631	0.311
4625	2.45	14.43	1.16	0.924	-0.10	+0.29	...	0.598	0.312
4750	2.70	14.88	1.61	0.869	-0.10	+0.29	...	0.547	0.310
4950	3.25	16.01	2.74	0.790	-0.10	+0.29	...	0.432	0.299
5150	3.76	17.13	3.86	0.722	-0.10	+0.29	...	0.308	0.281
5700	4.00	17.25	3.98	0.560	-0.10	+0.29	...	-0.006	0.185
5820	4.07	17.25	3.98	0.528	-0.10	+0.29	...	-0.049	0.156
5950	4.25	17.60	4.33	0.499	-0.10	+0.29	...	-0.078	0.131
5925	4.35	17.87	4.60	0.508	-0.10	+0.29	...	-0.068	0.140
5850	4.50	18.31	5.04	0.533	-0.10	+0.29	...	-0.036	0.163
5750	4.55	18.52	5.25	0.562	-0.10	+0.29	...	0.003	0.188
3825	0.90	12.05	-1.23	1.469	-0.30	+0.49	...	0.444	0.197
4050	1.30	12.53	-0.74	1.269	-0.30	+0.49	...	0.551	0.230
4250	1.70	13.14	-0.13	1.126	-0.30	+0.49	...	0.625	0.265
4500	2.20	13.98	0.71	0.985	-0.30	+0.49	...	0.613	0.281
4625	2.45	14.43	1.16	0.924	-0.30	+0.49	...	0.589	0.283
4750	2.70	14.88	1.61	0.869	-0.30	+0.49	...	0.547	0.280
4950	3.25	16.01	2.74	0.790	-0.30	+0.49	...	0.442	0.286
5150	3.76	17.13	3.86	0.722	-0.30	+0.49	...	0.325	0.245
5700	4.00	17.25	3.98	0.560	-0.30	+0.49	...	0.010	0.149
5820	4.07	17.25	3.98	0.528	-0.30	+0.49	...	-0.036	0.125
5950	4.25	17.60	4.33	0.499	-0.30	+0.49	...	-0.069	0.104
5925	4.35	17.87	4.60	0.508	-0.30	+0.49	...	-0.057	0.111
5850	4.50	18.31	5.04	0.533	-0.30	+0.49	...	-0.024	0.130
5750	4.55	18.52	5.25	0.562	-0.30	+0.49	...	0.019	0.151

TABLE 2A—*Continued*

T_{eff}	log g	V	M_V	$(B-V)_0$	[C/A]	[N/A]	[O/A]	S(3839)	s_{CH}
Group C									
3825	0.90	12.05	-1.23	1.469	-0.20	+0.61	-0.10	0.542	0.227
4050	1.30	12.53	-0.74	1.269	-0.20	+0.61	-0.10	0.685	0.254
4250	1.70	13.14	-0.13	1.126	-0.20	+0.61	-0.10	0.787	0.290
4500	2.20	13.98	0.71	0.985	-0.20	+0.61	-0.10	0.788	0.306
4625	2.45	14.43	1.16	0.924	-0.20	+0.61	-0.10	0.765	0.307
4750	2.70	14.88	1.61	0.869	-0.20	+0.61	-0.10	0.719	0.303
4950	3.25	16.01	2.74	0.790	-0.20	+0.61	-0.10	0.603	0.289
5150	3.76	17.13	3.86	0.722	-0.20	+0.61	-0.10	0.469	0.269
5700	4.00	17.25	3.98	0.560	-0.20	+0.61	-0.10	0.080	0.167
5820	4.07	17.25	3.98	0.528	-0.20	+0.61	-0.10	0.015	0.140
5950	4.25	17.60	4.33	0.499	-0.20	+0.61	-0.10	-0.033	0.117
5925	4.35	17.87	4.60	0.508	-0.20	+0.61	-0.10	-0.016	0.125
5850	4.50	18.31	5.04	0.533	-0.20	+0.61	-0.10	0.030	0.146
5750	4.55	18.52	5.25	0.562	-0.20	+0.61	-0.10	0.088	0.170
3825	0.90	12.05	-1.23	1.469	-0.30	+0.76	-0.20	0.568	0.225
4050	1.30	12.53	-0.74	1.269	-0.30	+0.76	-0.20	0.722	0.253
4250	1.70	13.14	-0.13	1.126	-0.30	+0.76	-0.20	0.833	0.287
4500	2.20	13.98	0.71	0.985	-0.30	+0.76	-0.20	0.839	0.301
4625	2.45	14.43	1.16	0.924	-0.30	+0.76	-0.20	0.818	0.300
4750	2.70	14.88	1.61	0.869	-0.30	+0.76	-0.20	0.772	0.295
4950	3.25	16.01	2.74	0.790	-0.30	+0.76	-0.20	0.654	0.279
5150	3.76	17.13	3.86	0.722	-0.30	+0.76	-0.20	0.516	0.256
5700	4.00	17.25	3.98	0.560	-0.30	+0.76	-0.20	0.105	0.151
5820	4.07	17.25	3.98	0.528	-0.30	+0.76	-0.20	0.034	0.126
5950	4.25	17.60	4.33	0.499	-0.30	+0.76	-0.20	-0.019	0.104
5925	4.35	17.87	4.60	0.508	-0.30	+0.76	-0.20	0.000	0.112
5850	4.50	18.31	5.04	0.533	-0.30	+0.76	-0.20	0.049	0.131
5750	4.55	18.52	5.25	0.562	-0.30	+0.76	-0.20	0.113	0.153
Group D									
3825	0.90	12.05	-1.23	1.469	...	+0.50	...	0.565	0.248
4050	1.30	12.53	-0.74	1.269	...	+0.50	...	0.725	0.271
4250	1.70	13.14	-0.13	1.126	...	+0.50	...	0.833	0.307
4500	2.20	13.98	0.71	0.985	...	+0.50	...	0.832	0.325
4625	2.45	14.43	1.16	0.924	...	+0.50	...	0.807	0.327
4750	2.70	14.88	1.61	0.869	...	+0.50	...	0.758	0.325
4950	3.25	16.01	2.74	0.790	...	+0.50	...	0.640	0.314
5150	3.76	17.13	3.86	0.722	...	+0.50	...	0.504	0.298
5700	4.00	17.25	3.98	0.560	...	+0.50	...	0.105	0.203
5820	4.07	17.25	3.98	0.528	...	+0.50	...	0.034	0.174
5950	4.25	17.60	4.33	0.499	...	+0.50	...	-0.020	0.147
5925	4.35	17.87	4.60	0.508	...	+0.50	...	-0.001	0.147
5850	4.50	18.31	5.04	0.533	...	+0.50	...	0.049	0.181
5750	4.55	18.52	5.25	0.562	...	+0.50	...	0.112	0.207

TABLE 2

B. Indices Derived from Synthetic Spectra

T_{eff}	log g	V	M_V	$(B-V)_0$	[C/A]	[N/A]	[O/A]	S(3839)	s_{CH}
Group A (with $^{12}C/^{13}C = 4$)									
3825	0.90	12.05	-1.23	1.469	...	...	...	0.528	0.254
4050	1.30	12.53	-0.74	1.269	...	...	...	0.675	0.276
4250	1.70	13.14	-0.13	1.126	...	...	...	0.757	0.314
4500	2.20	13.98	0.71	0.985	...	...	...	0.703	0.331
4625	2.45	14.43	1.16	0.924	...	...	...	0.647	0.333
4750	2.70	14.88	1.61	0.869	...	...	...	0.568	0.331
4950	3.25	16.01	2.74	0.790	...	...	...	0.415	0.319
5150	3.76	17.13	3.86	0.722	...	...	...	0.267	0.301
5700	4.00	17.25	3.98	0.560	...	...	...	-0.040	0.205
5820	4.07	17.25	3.98	0.528	...	...	...	-0.074	0.175
5950	4.25	17.60	4.33	0.499	...	...	...	-0.096	0.147
5925	4.35	17.87	4.60	0.508	...	...	...	-0.087	0.158
5850	4.50	18.31	5.04	0.533	...	...	...	-0.062	0.182
5750	4.55	18.52	5.25	0.562	...	...	...	-0.030	0.209
Group C (with $^{12}C/^{13}C = 4$)									
3825	0.90	12.05	-1.23	1.469	-0.30	+0.76	-0.20	0.583	0.229
4050	1.30	12.53	-0.74	1.269	-0.30	+0.76	-0.20	0.834	0.258
4250	1.70	13.14	-0.13	1.126	-0.30	+0.76	-0.20	0.995	0.293
4500	2.20	13.98	0.71	0.985	-0.30	+0.76	-0.20	1.030	0.307
4625	2.45	14.43	1.16	0.924	-0.30	+0.76	-0.20	1.012	0.306
4750	2.70	14.88	1.61	0.869	-0.30	+0.76	-0.20	0.958	0.301
4950	3.25	16.01	2.74	0.790	-0.30	+0.76	-0.20	0.804	0.284
5150	3.76	17.13	3.86	0.722	-0.30	+0.76	-0.20	0.623	0.259
5700	4.00	17.25	3.98	0.560	-0.30	+0.76	-0.20	0.123	0.151
5820	4.07	17.25	3.98	0.528	-0.30	+0.76	-0.20	0.045	0.126
5950	4.25	17.60	4.33	0.499	-0.30	+0.76	-0.20	-0.013	0.104
5925	4.35	17.87	4.60	0.508	-0.30	+0.76	-0.20	0.007	0.112
5850	4.50	18.31	5.04	0.533	-0.30	+0.76	-0.20	0.062	0.131
5750	4.55	18.52	5.25	0.562	-0.30	+0.76	-0.20	0.132	0.154

TABLE 2

C. Indices Derived from Synthetic Spectra

T_{eff}	log g	V	M_V	$(B-V)_0$	Mg_2	
					[Mg/A]=0.00	[Mg/A]=+0.25
3825	0.90	12.05	-1.23	1.469	0.276	0.322
4050	1.30	12.53	-0.74	1.269	0.202	0.243
4250	1.80	13.14	-0.13	1.126	0.151	0.186
4500	2.20	13.98	0.71	0.985	0.113	0.140
4625	2.45	14.43	1.16	0.924	0.102	0.126
4750	2.70	14.88	1.61	0.869	0.094	0.115
4950	3.25	16.01	2.74	0.789	0.089	0.109
5150	3.76	17.13	3.86	0.722	0.087	0.108
5700	4.00	17.25	3.98	0.560	0.058	0.069
5820	4.07	17.25	3.98	0.528	0.055	0.065
5950	4.25	17.60	4.33	0.499	0.053	0.063
5925	4.35	17.87	4.60	0.508	0.056	0.067
5850	4.50	18.31	5.04	0.533	0.062	0.075
5750	4.55	18.52	5.25	0.562	0.068	0.084

to ^{13}C abundances, both for MS and more luminous stars. As the effects of ^{13}C on the blue spectra of the 47 Tuc MS stars appear to be small, changes in $^{12}C/^{13}C$ ratios will not be considered further (see BBSH for a detailed discussion of the more luminous 47 Tuc stars). In a similar manner, the changes in synthetic CN MS band strengths with ξ are also expected to be small, as the bands are far from saturated. Calculations indicate that a change from $\xi = 1.0$ to 2.5 km s^{-1}, for a typical MS star (based on the $T_{eff} = 5930$ K, log $g = 4.30$ model and both the CN strong and weak cases) will result in a change in the derived $S(3839)$ index of 0.014 (or $\sim 0.4\ \sigma$, see below). Similarly, the s_{CH} index should shift by 0.017 (1 σ). Overall, these differ-

TABLE 3

Regions Used in Flux Normalizations

Region	Start Wavelength (Å)	End Wavelength (Å)
1..........	3700	3750
2..........	3750	3800
3..........	3800	3825
4..........	3916	4000
5..........	4000	4050
6..........	4050	4150
7..........	4150	4220
8..........	4220	4280
9..........	4320	4350
10..........	4350	4400
11..........	4400	4450
12..........	4450	4500
13..........	4500	4550
14..........	4550	4600
15..........	4600	4650
16..........	4650	4700
17..........	4700	4750
18..........	4750	4800
19..........	4800	4850
20..........	4850	4890
21..........	4958	5000
22..........	5000	5050
23..........	5050	5100
24..........	5100	5160
25..........	5200	5250
26..........	5250	5300
27..........	5370	5400
28..........	5400	5450

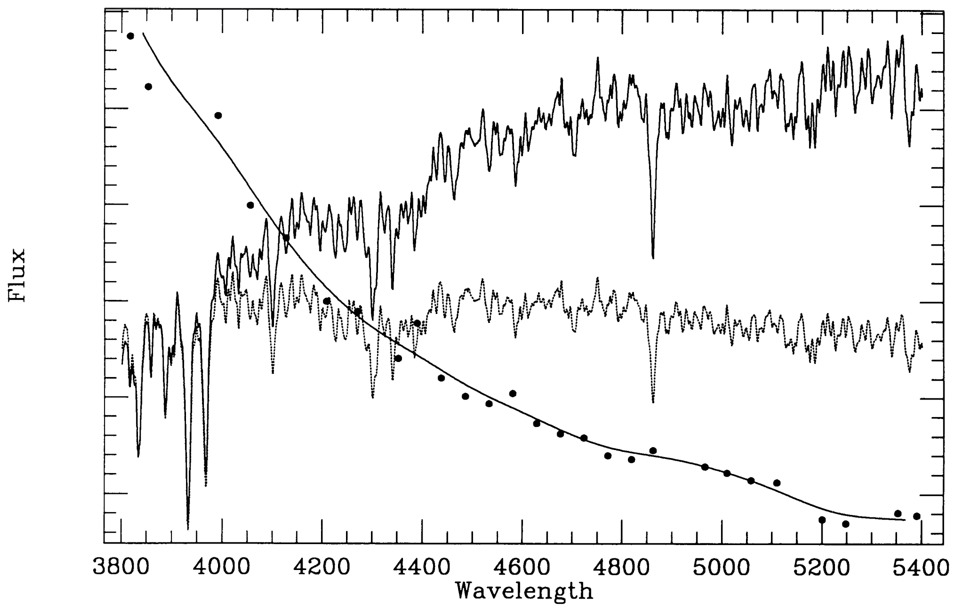

FIG. 2.—A sample observed spectrum before (*solid line*) and after the slope correction (*dotted line*). The correction function is also shown, with the filled circles marking correction factors determined for the regions in Table 3.

TABLE 4

WAVELENGTH RANGES FOR F_λ CALCULATIONS

Mean Flux	Wavelength Range (Å)	Feature
$F_{\lambda,\mathrm{FCN}}$	3846–3883	3883 Å CN band
$F_{\lambda,\mathrm{CCN}}$	3883–3916	3883 Å CN continuum
$F_{\lambda,\mathrm{FCH}}$	4280–4320	CH G band
$F_{\lambda,\mathrm{CCH1}}$	4220–4280	CH G band continuum
$F_{\lambda,\mathrm{CCH2}}$	4400–4480	CH G band continuum
$F_{\lambda,\mathrm{FMG}}$	5160–5197.25	MgH + Mg *b* features
$F_{\lambda,\mathrm{CMG1}}$	4897–4958.25	Mg continuum
$F_{\lambda,\mathrm{CMG2}}$	5303–5366.75	Mg continuum

ences in the indices will translate into abundance differences of ~0.1 in both [C/A] and [N/A].

4. RESULTS

4.1. CN *Band Strengths*

The $S(3839)$ indices from both the observed and synthetic spectra are plotted together in Figure 4. Large variations in the CN band strengths can be seen over the range $1 < M_V < 5.5$. This is illustrated further in Figure 5, where the spectra of two $M_V = +4.4$ stars, observed simultaneously, have been plotted together. In Figure 6, the spectra for stars H-20030, 20032, 20034, 10023, 20053, and 20068 have been averaged together

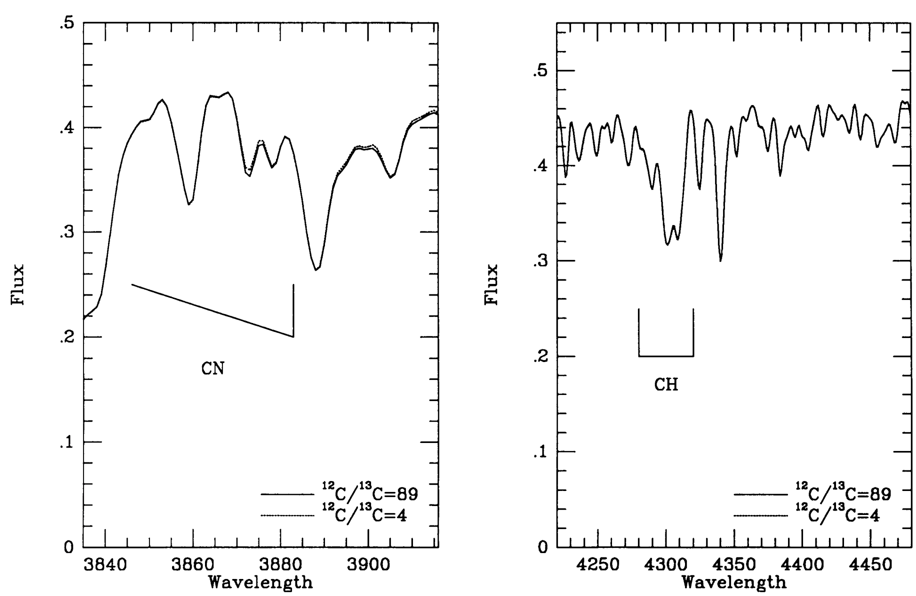

FIG. 3.—Synthetic spectra from the $T_{\mathrm{eff}} = 5925$ K, log $g = 4.35$ model with solar [C, N, O/A] have been plotted with ^{12}C/^{13}C ratios of 89 and 4 for the regions appropriate to the $S(3839)$ and s_{CH} indices. There is little additional absorption in either band with an increase in ^{12}C/^{13}C. This is quite different to the case of the cooler stars (see Fig. 3 of BBSH).

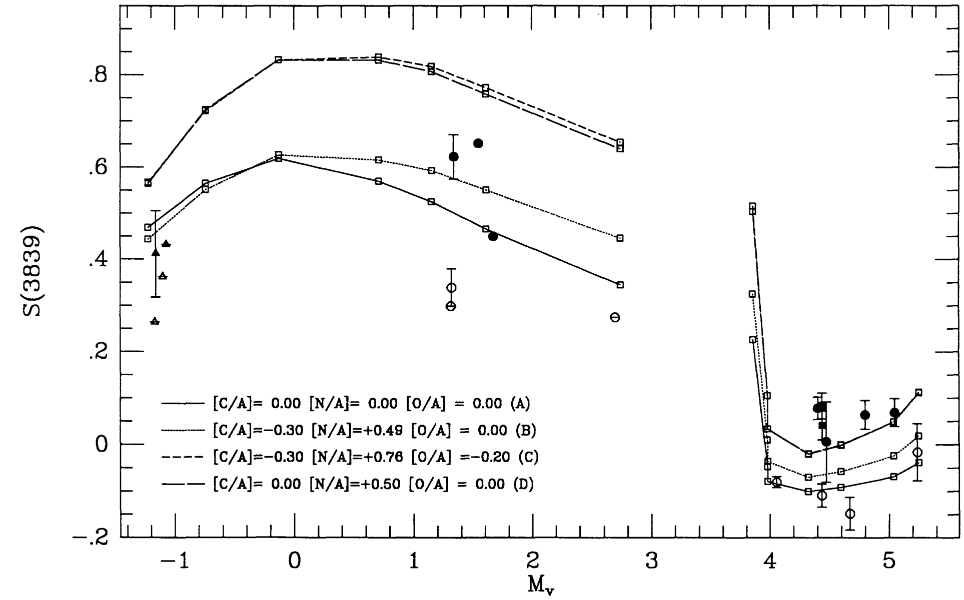

FIG. 4.—The S(3839) indices have been plotted for all observed stars and the synthetic spectra of Table 2 (same symbols as in Fig. 1). Note that there are significant differences in the 3883 Å CN band strengths over the entire 6 mag observed (although the $M_V = -1$ bands have saturated).

and plotted against the average of stars H-10014, 20033, 20045, and 20083; the former being CN-strong and the latter CN-normal. As in Figure 5, the differences in CN band strengths are very apparent (note how similar all the other features are in these two averaged spectra, as would be expected from the small dispersion in $B-V$ color of 47 Tuc's CM-diagram). These figures are similar to comparisons made by Hesser & Bell (1980) and Bell, Hesser, & Cannon (1983). Moreover, inspection of Figure 5 and the spectral indices in Table 1 for paired stars, shows that ranges of S(3839) in excess of the observed errors exist among the pairs. As a further check of the observations, the spectrum from each program star was also visually compared to the preliminary data from the AAT fiber run with the result that CN-strong stars appeared to be CN-strong in both data sets. Consequently this work both confirms, and extends to somewhat fainter stars, the earlier results of Hesser & Bell (1980) and Bell, Hesser, & Cannon (1983) *that variations in* 3883 Å CN *band strengths exist on the 47 Tuc upper MS.*

The subgiants were observed largely for comparisons with the data of SBH and BBSH. In Figure 7, the S(3839) indices for the two data sets are plotted together. Note that BBSH did not employ any slope corrections, and both sets of observations were obtained using a slit size which was smaller than the seeing disks. This is thought to enhance the effects of differential refraction which are hypothesized to be the cause of the

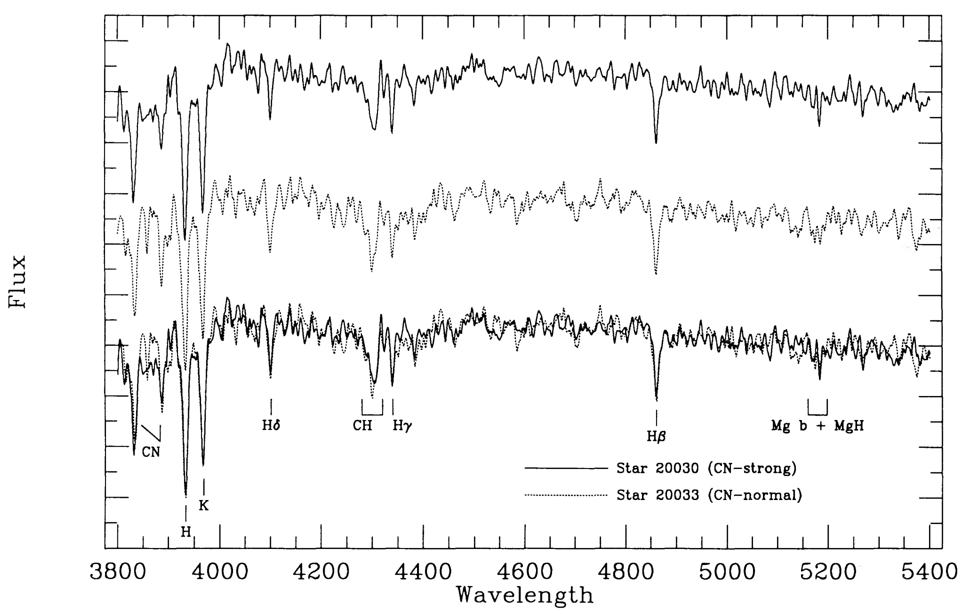

FIG. 5.—Two 47 Tuc MS stars (20030 and 20033), observed simultaneously, having very similar colors and brightnesses, appear to have markedly different 3883 Å CN band strengths (the continua of these spectra have been corrected by the procedure described in § 3).

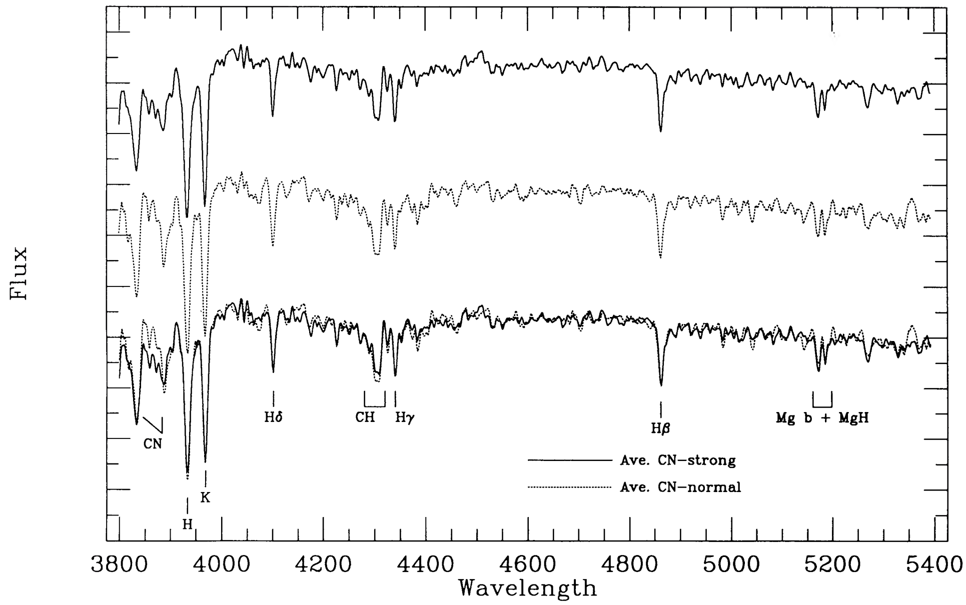

FIG. 6.—The spectra for stars H-20030, 20032, 20034, 10023, 20053, and 20068 (all CN-strong) have been averaged and plotted against the average spectrum from stars H-10014, 20033, 20045, and 20083 in order to improve the S/N and thereby better illustrate the differences in 3883 Å band strengths as well as similarities in other features.

slope uncertainties in the present data. Thus, it is not clear which of the two runs would be most affected by this problem. While the present observations give essentially the same result as the previous study for four of the stars, the indices differ by slightly less than 0.2 for the remaining two. However, even if the present data are correct, this does not affect the conclusions of SBH or BBSH.

As the subgiant CN band strengths are discussed in great detail in SBH and BBSH, they will not be covered further in this paper, except to note that it would appear that a small zero point difference remains between the observed and synthetic $S(3839)$ indices for the subgiants and brighter stars. This is more apparent for the $M_V = -1$ stars, in which the 3883 Å CN bands are much stronger than for the $M_V = 1.5$ stars. BBSH found that a shift of -0.15 for the synthetic $S(3839)$ indices was necessary in order to fit the observations in their sample of 47 Tuc subgiants. From an examination of Figure 4, such a shift would also bring the present indices into better agreement.

For the MS stars ($M_V > 4$), the range in $S(3839)$ is of order 0.2 mag, or 5–6 σ [$\sigma = 0.036$ being the average error in $S(3839)$]. This is quite consistent with SBH and BBSH, who found differences of 5–8 σ in the 4215 Å CN bands, and a spread of 0.55 mag, or 11 σ ($\sigma = 0.05$) in the 3883 Å bands of 47 Tuc subgiants (note from Fig. 4 that the sensitivity of $S(3839)$ to changes in CN abundance is expected to be some 3 times greater for the subgiants than for the MS stars).

A comparison between the observed and synthetic MS S(3839) indices (Fig. 4) shows that the solar C, N, and O synthetic spectra provide a fairly reasonable baseline to the CN normal MS stars (with the possible exception of star H-20045). However, the group (B) MS spectra, which are calculated for [C/A] = -0.3, [N/A] = $+0.49$ and give the strongest possible CN bands for the mixing of C → N-process material, do not match the range in CN strengths observed. Further mixing of C → N-process material (holding C + N constant) will not increase the strengths of the CN bands (Smith & Bell 1986). Thus, *the mixing of* C → N-*process material into an atmosphere with initial* C *and* N *abundances in the solar ratio cannot account for the present observations* (the effect of a higher assumed [A/H] for 47 Tuc is discussed in § 4.4). With the mixing of O → N-processed material into the atmosphere; the range in CN band strengths can be better matched, since the N abundance can be enhanced for a much smaller depletion of C, although a different ratio of mixed C → N to O → N-processed material than was used in the calculations is necessary. A similar requirement of O → N-processed material mixing was

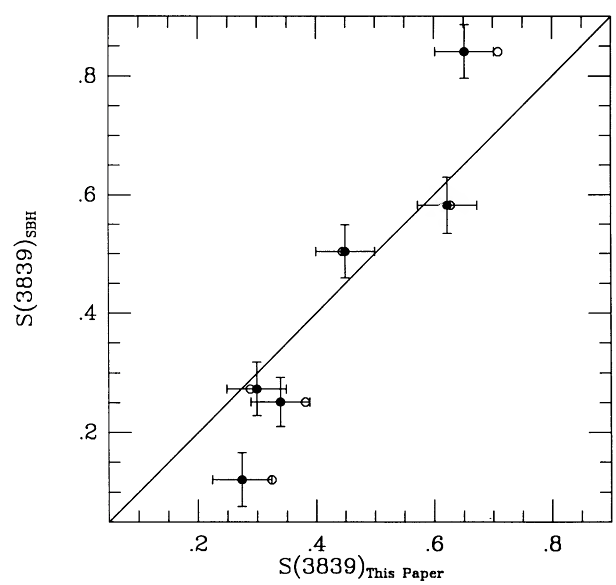

FIG. 7.—$S(3839)$ values for stars in common with BBSH and this work have been plotted against each other. The open circles represent $S(3839)$ indices as measured from the observed spectra prior to any corrections in the continua shape, while the closed circles are indices from the slope corrected data. The error bars from BBSH were taken from the estimate in their text (0.05). Note that the slope from the data is slightly less than unity (the solid line is a one-to-one correlation).

found by SBH, from the 4215 Å CN bands of the subgiants. However, for the observed MS stars, very little atmospheric C is bound up in CO. Thus, a reduction of the O abundance does not appreciably increase the amount of free C, contrary to the case for the cooler stars (SBH). Synthetic spectra yield $S(3839) = 0.072$ for a $T_{\rm eff} = 5850$, $\log g = 4.50$, $[A/H] = -0.8$ atmosphere with $[C/A] = -0.15$, $[N/A] = +0.70$, and $[O/A] = 0.0$. The value of $S(3839)$ changes by only 0.003 when O is reduced by 0.2. An increase in $[O/A]$ of 0.35, as has been suggested by the isochrone fits of Hesser et al. (1987), will result in $S(3839) = 0.061$ (using the same $[C/A]$ and $[N/A]$). The 0.011 difference in $S(3839)$, although larger than the result from decreasing $[O/A]$, is still 3 times smaller than the average error in $S(3839)$ for a MS star.

A variation in overall nitrogen abundances can also produce the range of $S(3839)$ observed in the MS stars (Fig. 4). The $[N/A] = +0.5$ synthetic spectra almost match the $[C/A] = -0.3$, $[N/A] = +0.76$, $[O/A] = -0.2$ spectra in 3883 Å CN band strengths. Further modeling shows that a spread of 0.7 in $[N/A]$ alone would match the $S(3839)$ observations (assuming no overall carbon depletions or variations). A similar finding was obtained by Hesser & Bell (1980) and Bell, Hesser, & Cannon (1983) from low-resolution CTIO SIT vidicon spectra of SGB and upper MS stars.

The quantity $\delta S(3839)$, a measure of the additional 3883 Å CN absorption as compared to a synthetic spectrum with $[C, N/A] = 0.0$, is defined as

$$\delta S(3839) = S(3839)_{\rm obs} - S(3839)_{{\rm synth(C,N=\odot)}} .$$

This quantity possess the advantage of having the temperature contribution of the CN band strength index removed through the subtraction of the synthetic index. $\delta S(3839)$ was computed for all stars with $M_V > 4$. The values of $S(3839)_{{\rm synth(C,N=\odot)}}$ were evaluated at the M_V of each observed star with the use of cubic splines, computed from the synthetic spectra in group (A). The results for $\delta S(3839)$ are given in Table 1, and plotted in Figure 8, where each $\delta S(3839)$ value has been replaced by a Gaussian with unit area and a FWHM equal to the 1 σ error in that observation. The sample of 10 stars is too small for definitive conclusions and most certainly suffers from selection effects, but the figure appears to hint at a bimodality similar to the distribution observed on the HB, AGB, RGB, and SGB (see § 1). Such a bimodal distribution among the MS stars would therefore be indicative of a true bimodality in CN abundance, as the 3883 Å bands in the MS stars are not saturated.

4.2. CH *Band Strengths*

The G-band sensitive index, $s_{\rm SCH}$, has been plotted in Figure 9. Note that for the MS synthetic spectra, little difference is seen between the $s_{\rm CH}$ indices for $[O/A] = 0.0$ and -0.2, with $[C/A] = -0.3$. This is due to the weakness of the CO bands on the MS, as mentioned earlier. The $s_{\rm CH}$ indices are compared with those of SBH in Figure 10, where problems similar to those in Figure 7 can be seen. Star AW-3, which has the lowest $s_{\rm CH}$ value of all the stars in SBH, appears to be somewhat less carbon poor in this analysis. Again, the subgiants have already been analyzed in great detail by SBH and BBSH.

There is a smaller range in the CH index variations (of order 0.05, or 3–4 σ, $\sigma = 0.018$, the average error) for the MS stars than in the CN indices. The calculations suggest that this is the result of a smaller range in C abundances: most of the stars are clearly within $+0.1 < [C/A] < -0.3$ (the notable exceptions being stars 10014 and 20053). Hesser (1978) reported no evidence for CH variations on the MS, from very low resolution spectra. Bell, Hesser, & Cannon (1983) derived either $[C/A] = 0.0$ or -0.2 from their sample of MS stars.

In a manner analogous to $\delta S(3839)$, $\delta s_{\rm CH}$ was computed for the MS stars. The resulting values may be found in Table 1, and are plotted, against the $\delta S(3839)$ indices in Figure 11. With the two indices being defined in such a way as to remove the temperature contributions, and with the indices' sensitivities to abundance changes being relatively constant over the observed

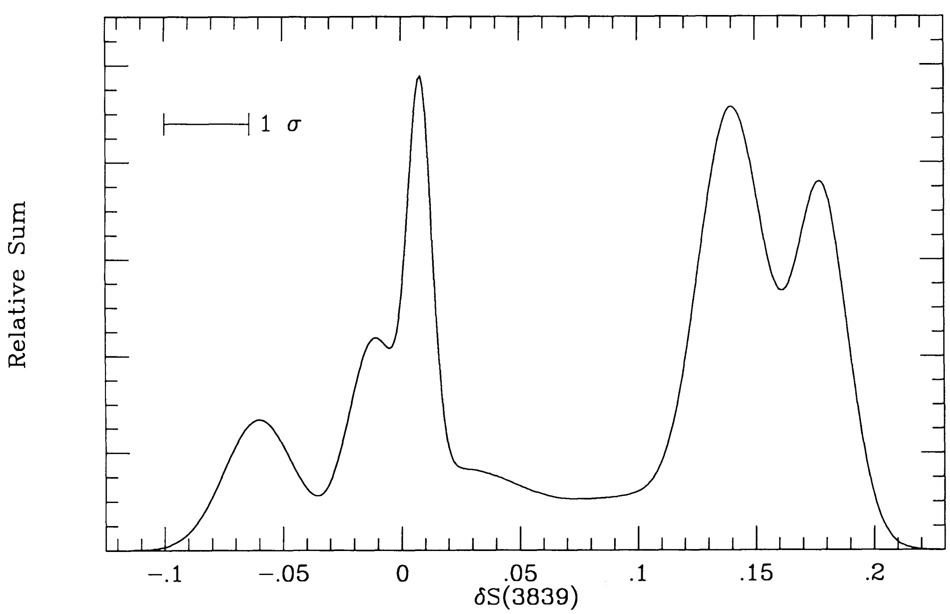

FIG. 8.—The distribution of $\delta S(3839)$ is plotted, where each $\delta S(3839)$ point has been replaced by a Gaussian with unit area and a FWHM equal to the error in that observation. Thus the observations with the larger error bars are weighted less in the computation of the sum of the Gaussians at each point. Although 10 stars is clearly an insufficient sample, the resulting distribution hints at a bimodality similar to that seen in the more luminous 47 Tuc stars.

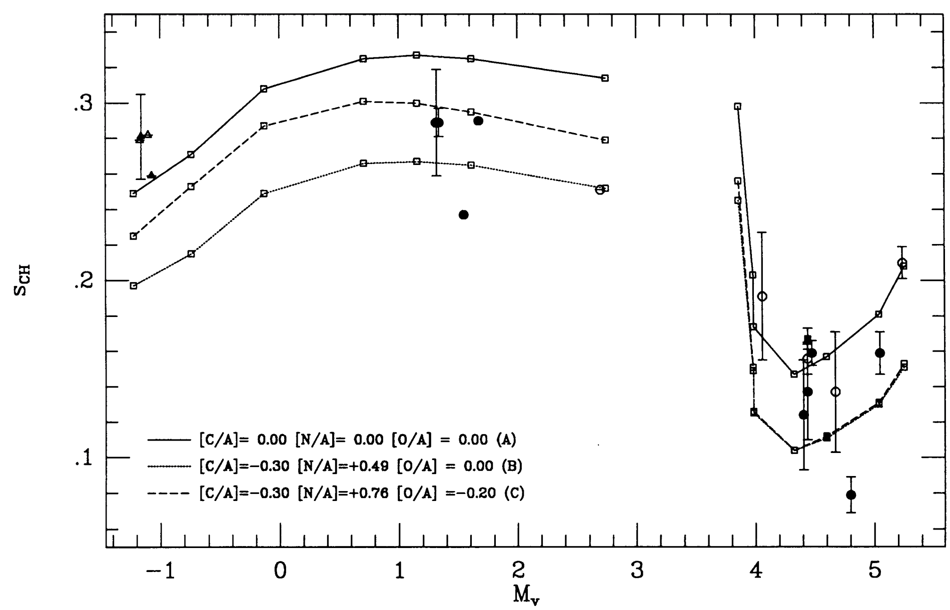

FIG. 9.—The s_{CH} indices from both the observed and synthetic spectra have been plotted over the entire range in M_V (the markers are as in Fig. 1). Note the difference between group (A) and (C) on the SGB and RGB. By the MS, the CO formation has become so weak that O abundance has little effect on CH band strength.

interval, Figure 11 should reveal whether or not a CN/CH anticorrelation (such as might be expected were mixing processes responsible for the range of CN and CH band strengths) is present in the data. Such anticorrelations have been observed on the HB (Norris & Freeman 1982), AGB (Norris & Cottrell 1979), RGB (Norris, Freeman, & DaCosta 1984), and SGB (SBH, only in the CN-strong stars). In the case of an anticorrelation, the CN-normal stars should cluster in the upper-left portion of the diagram, and the CN-strong in the lower-right portion. No such trend appears to be evident, but the errors in the G-band observations of individual faint stars are significant (i.e. $\langle \delta s_{CH} \rangle = 0.004 \pm 0.010$ (s.d.m.) and -0.013 ± 0.017 for the two groups, while $\langle \delta S(3839) \rangle = -0.912 \pm 0.018$ and 0.147 ± 0.012, respectively). Figure 6 also serves to emphasize the significance of errors in this analysis: although an anticorrelation between CN and CH is suggested by the similar behavior of the 4325 Å CH + Fe I feature and the G band, the differences appear to be of the order of other variations which may be attributed to noise (i.e., the 4352–4384 Å Fe I region, which are assumed to be intrinsically the same in both averaged spectra). To convincingly demonstrate a CN, CH anticorrelation will require substantially higher signal to noise in the individual spectra.

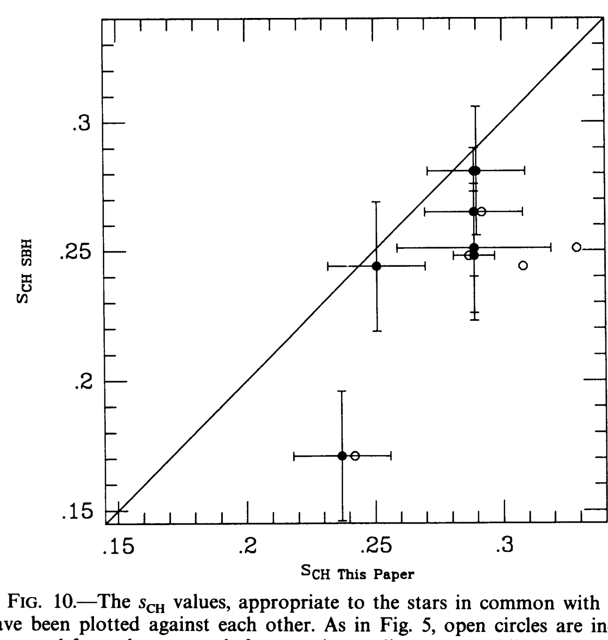

FIG. 10.—The s_{CH} values, appropriate to the stars in common with SBH have been plotted against each other. As in Fig. 5, open circles are indices measured from the spectra before continua adjustments, while closed circles indicate results from the slope corrected data. The line has unity slope, and the error bars for the SBH data come from their text. Note that star AW-3 has the lowest s_{CH} index of all the SBH subgiants.

4.3. Mg_2 *Indices*

Other investigators have found a correlation between Na atomic line and CN band strengths (Cottrell & Da Costa 1981; Lloyd Evans, Menzies, & Smith 1982). Cottrell & Da Costa also searched for corresponding variations in Mg strengths but found none. In order to extend their Mg analysis to the MS, the Mg_2 index of Faber et al. (1985) was measured from the observed and synthetic spectra. The bandpass contains the 5177 Å Mg *b* triplet. MgH lines are unlikely to be seen, owing to the relatively high T_{eff} values of the MS stars, and the low surface gravities of the cool red giants. The results are plotted in Figure 12, where it may be seen that there is no correlation between Mg_2 and CN band strengths to within the measured errors. Continuous lines, connecting Mg_2 indices computed from synthetic spectra with [Mg/A] = 0.0 (the logarithmic solar Mg abundance taken to be 7.44), and [Mg/A] = +0.25 are also plotted. Adopting the value of [M/H] = −0.8 for 47 Tuc, and assuming that there are no zero point shifts in the Mg_2 indices, Figure 12 appears to indicate a Mg overabundance for 47 Tuc slightly larger than the +0.1 dex seen by Cottrell & Da Costa.

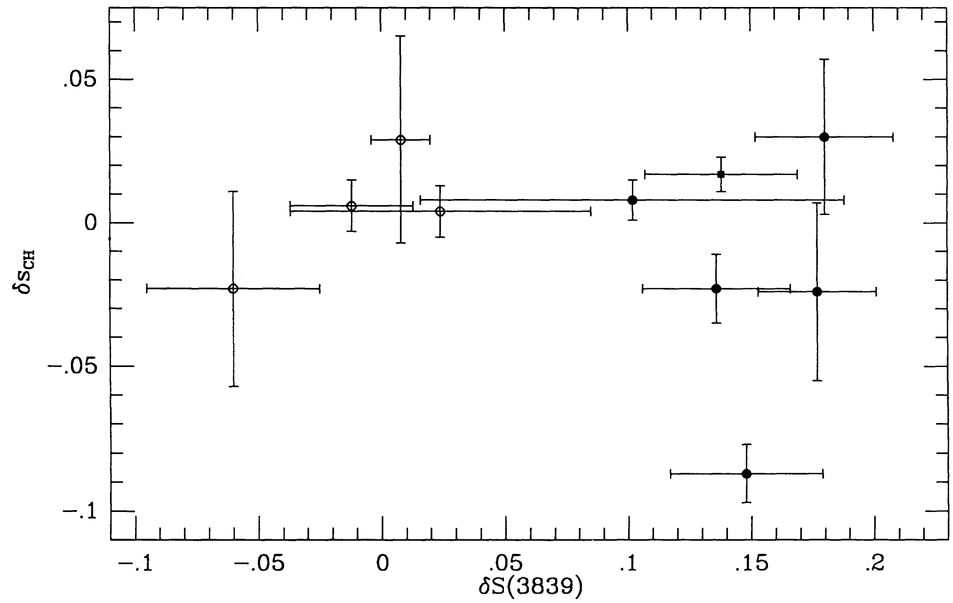

FIG. 11.—Values of $\delta S(3839)$ have been plotted against δs_{CH} for the MS stars (same symbols as in Fig. 5). In the case of a CN/CH anticorrelation, the CN-normal stars should be in the upper-left hand corner, while the CN-strong stars should be in the lower-right hand corner. Although no such trend is seen, these are faint stars, and the associated errors are large.

4.4. *The* C *and* N *Abundance Ranges*

In Figure 5, spectra for a pair of stars observed simultaneously were overplotted and found to convincingly demonstrate the existence of a range of CN band strengths among the upper MS stars in 47 Tuc; other pairs show the same effect (see, e.g., Table 1). Having eliminated many possibilities of observational errors resulting in spurious CN variations (such as differences in instrumental response, sky subtractions, or data reduction procedures) by making simultaneous observations (see Fig. 5), thereby gaining confidence in the existence of a range, we now turn to analysis of representative CN-strong and normal stars.

Taking averages of the $\delta S(3839)$ and δs_{CH} values for the CN-strong stars, as presented in Figure 11, results in $\delta S(3839) = 0.147 \pm 0.012$ (s.d.m.) and $\delta s_{CH} = -0.013 \pm 0.017$. Similarly, for the CN-strong group, the averages are $\delta S(3839) = -0.010 \pm 0.018$ and $\delta s_{CH} = 0.004 \pm 0.010$.

These mean values for the two groups are fortuitously close (within 1 σ) to the observed stars H-20068 [$\delta S(3839) = 0.136 \pm 0.030$ and $\delta s_{CH} = -0.023 \pm 0.012$] and H-20033 [$\delta S(3839) = -0.012 \pm 0.025$ and $\delta s_{CH} = 0.006 \pm 0.009$]. Thus, these two stars will be considered representative of the CN-strong and CN-normal groups, respectively. Note that while it may appear from the two averages that an

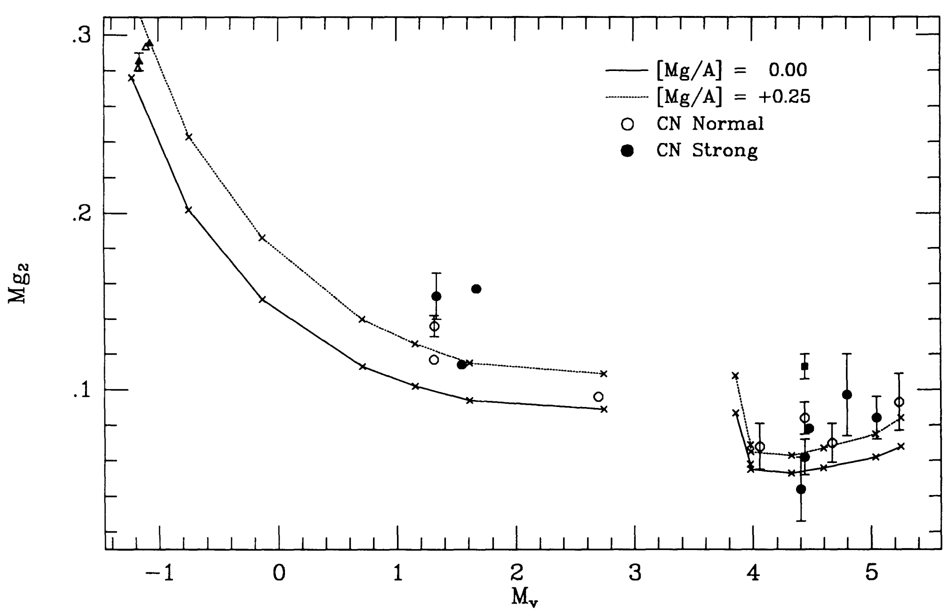

FIG. 12.—The Mg_2 index, as measured from both the observed and synthetic spectra is plotted (see Fig. 1 for the symbol key). No correlation between CN band strength and Mg_2 is apparent; however, it would appear that the 47 Tuc stars are slightly overabundant in Mg.

anticorrelation between CN and CH indeed exists, the errors in the s_{CH} indices are much greater than the difference in δs_{CH} between the two groups.

Calculations show that the $S(3839)$ and s_{CH} indices for the CN strong star H-20068 can be matched, to within the errors, by a synthetic spectrum computed from the $T_{eff} = 5850$ K, $\log g = 4.50$ model with [C/A] = −0.17 and [N/A] = +0.70 ($S(3839) = 0.069$, $s_{CH} = 0.152$). Again, the O abundance will have little effect on the amount of free C available for CH and CN formation. Similar calculations for the CN-normal star 20033, using a $T_{eff} = 5930$ K, $\log g = 4.30$ model, indicate that [C/A] = +0.01 and [N/A] = −0.18 will reproduce the observed $S(3839)$ and s_{CH} indices ($S(3839) = -0.109$, $s_{CH} = 0.155$). Thus, there appears to be a difference of about −0.2 in Δ[C/A] and +0.9 in Δ[N/A] (Δ[X/A] being defined as

$$[X/A]_{\text{CN-strong}} - [X/A]_{\text{CN-normal}})$$

between the two stars. Should the overall metallicity of 47 Tuc be somewhat greater than −0.8 dex, such as the [Fe/H] of −0.65 used for the isochrones in Hesser et al. (1987), the values for Δ[C/A] and Δ[N/A] will be slightly smaller. Using [A/H] = −0.65 and the appropriate models for H-20068 ($T_{eff} = 5910$ K and $\log g = 4.50$) and H-20033 ($T_{eff} = 5975$ K and $\log g = 4.30$) yields Δ[C/A] = −0.1 and Δ[N/A] = +0.8.

As far as abundance differences between these two individual stars are concerned, the abundance spread should be accurate to ±0.1 in C and ±0.2 in N. However, given the uncertainties in the average values of $\delta S(3839)$ and δs_{CH} for the entire group of stars, the errors are roughly ±0.2 for both C and N. Thus, the range in C and N for the MS stars in this sample may be roughly characterized by Δ[C/H] = −0.2 ± 0.2 and Δ[N/H] = +0.9 ± 0.2 (using [A/H] = −0.8). This is quite similar to the range of −0.2 for Δ[C/H] and +1.0 for Δ[N/H] derived by Norris & Cottrell (1979) from two 47 Tuc AGB stars, as well as the Δ[C/A] = −0.3, with Δ[N/A] = +0.9, found in 17 47 Tuc HB stars by Norris & Freeman (1982). Bell, Hesser, & Cannon (1983) found Δ[C/A] = −0.2 and Δ[N/A] = 0.5 among their sample of 47 Tuc MS stars. The four RGB tip stars (HH-2006, 2077, 3027, and 3205) were observed in the region of the 2.3 μm CO bands by Bell, Briley, & Smith (1990). They found that with $^{12}C/^{13}C = 5$ and 3 (respectively) for the CN-strong stars HH −2006 and 3027, and $^{12}C/^{13}C = 7$ and 8 for the CN-normal pair (HH −2077 and 3205), an average difference in [C/A] of 0.32 dex between the CN-strong and normal stars. These results were based on a ξ of 2.5 km s^{-1}, and as the CO bands are somewhat saturated for these stars, there is a strong dependence of band strength on ξ. Using 2.0 km s^{-1} for ξ yielded somewhat greater C abundances and $^{12}C/^{13}C$ ratios, but failed to reproduce the observed s_{CH} indices.

If the assumption is made that the results from the CN-normal star H-20033 represent the original C and N abundance of the cluster, and O is in the solar ratio, then a change in O abundance for star 20068 of as much as −0.2 (depending on the errors assumed) would be required in order to maintain constant C + N + O. Likewise, if it is assumed that the C and N abundances of star 20033 are in the solar ratio, some change in surface [O/A] of star 20068 must take place. Thus, in order to conserve the total surface C + N + O, as is required for any mixing mechanism (note that in this case, turbulent diffusion and gravitational settling are not considered true "mixing" mechanisms), some dredge-up of O → N processed material must take place in the transformation of star 20068 into a CN-strong star (note that in using [A/H] = −0.65, the mixing of C → N-processed material alone still cannot account for the observed CN and CH range). The same conclusion was also reached by SBH in their analysis of CN and CH in SGB stars. Unfortunately, such deep mixing is very difficult to explain in main-sequence stars (VandenBerg & Smith 1988 and references therein). However, Norris & Cottrell (1979) suggest that the protocloud from which 47 Tuc formed was N poor, by a factor of 4 after recalibration to [Fe/H] = −0.8. Should this be the case, an initial C over-abundance of +0.12 dex in 47 Tuc would allow both stars 20068 and 20033 to evolve to their present CN abundances, while conserving [(C + N)/Fe] (no change in O need be considered). Langer, Kraft, & Friel (1985) suggest a shift of +0.2 in [C/Fe] and −0.2 in [N/Fe] in order to maintain [(C + N)/Fe] in their sample of six M5 giants. Similarly, for the present data, a shift of +0.20 in [C/A] and −0.28 in [N/A] would do the same for the 47 Tuc MS stars. Note, however, that both of these proposals then require that the CN-normal stars also be mixed to some extent. Some mixing of the CN-normal stars is possible, as Bell, Briley, & Smith (1990) have detected strong ^{13}CO absorption in two 47 Tuc CN-normal RGB stars. However, these stars are bright giants which may have undergone a later mixing epoch on the RGB or SGB (BBSH). The idea that the CN-normal MS stars may be stars which have "supermixed" to the point where C → N-processing has produced abundances of C < N, giving weaker CN bands, is precluded by the G-band strengths.

5. DISCUSSION

It appears that there is a substantial difference between 47 Tuc and the field in terms of the relative numbers of CN-strong and normal stars (Hesser, Hartwick, & McClure 1976, 1977). The large surveys of field dwarf stars by Clegg, Tomkin, & Lambert (1981), Tomkin & Lambert (1984), Laird (1985), and Carbon et al. (1987) generally resulted in [N/Fe] ≈ 0.0 for −2 < [Fe/H] < +0.3 (there are some questions as to absolute values of [N/Fe] between the studies, but scatter in [N/Fe] at any given [Fe/H] is noticeably absent in every work). There would appear to be only a small (5%) number of N-rich stars in the samples of Laird & Carbon *et al.* Spite & Spite (1986) determined the Li abundances of four of these stars and thereby showed that the N enhancement cannot be the result of deep convective mixing. This indicates a primordial origin for the N overabundances in the field.

Significant numbers of CN-strong and normal stars are seen on the subgiant and giant branches of many clusters. Of the 12 clusters examined by Norris (1987, and references therein), nine were found to have larger numbers of CN-strong stars than CN-normal, and the cluster with the fewest CN-strong stars still had a ratio of 0.22 (number CN-strong/number CN-normal). While 47 Tuc was not in Norris's sample, it has been generally found to possess a roughly equal number of both CN-strong and normal stars on the AGB, HB, and RGB (Norris 1978; Norris & Freeman 1982; Norris, Freeman, & Da Costa 1984). BBSH found 16 CN-strong and 10 CN-normal stars on the 47 Tuc SGB. This in definite contrast to the 5% CN-strong stars found in the field and may be indicative of a different chemical history for the cluster stars. It should further be noted that the presence of CN abundance variations similar to those seen in 47 Tuc have never been ruled out for the most metal-poor clusters. This may largely be attributed to the overall weakness of the CN bands which are not visible at all in the metal poor clusters. Indeed, in the CH and NH studies of M92 (Carbon et al. 1982) and M15 (Trefzger et al. 1983) it was found that stars at the same position on the CMD exhibit differences in nitrogen abundances of a factor of 10, as well as variations of a factor of 3 in carbon (quite similar to the typical bimodal CN cluster results). As nitrogen abundances are relatively small and do not contribute much to the overall opacities, primordial variations in N are not expected to have a significant effect on CMD morphology. A difference of 0.7 in [N/A] for 47 Tuc should produce a difference in isochrones of ~ 0.3 Gyr (VandenBerg 1985).

Population I giants and metal-poor cluster red giants do, almost unequivocally, show evidence of mixing (Smith 1987; VandenBerg & Smith 1988; Wheeler, Sneden, & Truran 1989, and references therein). Depletions of carbon and enhancements of nitrogen have been observed in Population I giants by Lambert & Ries (1981) ([C/Fe] = -0.24 with [N/Fe] = $+0.35$ from 32 stars) and Kjaergaard et al. (1982) ([C/Fe] = -0.26 and [N/Fe] = $+0.10$). Most of the differences in the two determinations are explained by Kjaergaard et al. as being due to their adoption of systematically lower stellar temperatures. The most metal-poor clusters ([Fe/H] < -2), M92, M15, and NGC 6397, show a very strong dependence of carbon depletion on luminosity, with the most luminous stars reaching [C/A] = -0.7 or more (Bell, Dickens, & Gustafsson 1979; Carbon et al. 1982; Trefzger et al. 1983; and Briley et al. 1990). Bell & Dickens (1980) also find that carbon is depleted, but by a much smaller amount, in the brightest giants of the more metal rich clusters M3, M13, and NGC 6752 ([Fe/H] = -1.5). Observations by Smith & Suntzeff (1990) have further indicated a decrease in [C/A] with luminosity (of order 0.4 dex) on the NGC 6752 (a CN-bimodal cluster) giant branch. Yet, in the case of 47 Tuc, SBH show that the variation of carbon depletion with luminosity seen in the metal-poor clusters cannot occur in 47 Tuc, as it would imply CN band strengths which are much weaker than those observed. This would appear to be in agreement with the suggestion of Bell & Dickens (1980) that the extent of the RGB carbon depletions is correlated with metallicity (the more metal-poor clusters suffering from the largest depletions). That some mixing occurs on the 47 Tuc RGB seems likely though, as $^{12}C/^{13}C$ ratios as low as 4–13 have been observed in 47 Tuc RGB tip stars (Brown & Wallerstein 1989; Bell, Briley, & Smith 1990), regardless of their CN band strengths.

The preceeding discussion suggests that powerful constraints could be placed on globular cluster chemical evolution were it possible to increase the sample size of spectroscopically observed stars, including on the MS, and decrease the error bars.

6. CONCLUSIONS

Moderate resolution spectra (≈ 4.0 Å FWHM) of the blue CN and CH bands of 10 MS, six SGB, and four RGB tip stars in 47 Tuc have been obtained. Star-to-star differences in CN and CH band strengths have been found to occur among stars which have not yet evolved past the MS turn-off, in confirmation of the earlier results of Hesser (1978), Hesser & Bell (1980) and Bell, Cannon, & Hesser (1983). The range of variations was quantified using the $S(3839)$ and s_{CH} indices applied to observed and synthetic spectra.

The range in $S(3839)$ is ~ 0.2 mag (5–6 σ), which is very consistent with the range in $S(3839)$ seen by BBSH in SGB stars. The distribution of 3883 Å CN band strengths in these stars is suggestive of a continuation of the CN bimodality which has already been observed throughout the other more evolved branches of the CM-diagram. The s_{CH} index also varies by ~ 0.05 mag (3–4 σ). The errors in the observations are too large for the detection of an overall CN/CH anticorrelation, as has been observed in the cooler, more evolved stars (if anything, our data suggest little to no anticorrelation).

Indices for the CN-normal stars are well matched by synthetic spectra with C abundances near the solar ratio and a small N deficiency ([N/A] ≈ -0.2). The CN-strong stars compare well to synthetic spectra with a slight C deficiency ([C/A] ≈ -0.2) and a N overabundance ([N/A] $\approx +0.7$). Changes in the O abundances of the MS stars should have little impact on the CN and CH band strengths. A difference of about -0.2 ± 0.2 in [C/A] and $+0.9 \pm 0.2$ in [N/A] seems reasonably representative of the range among the MS stars and is consistent with the range found by others among cooler, more luminous, 47 Tuc stars.

The results for the CN-strong stars cannot be readily matched by the assumed mixing of C $\rightarrow$ N-process material (C + N = constant) and initial cluster C and N abundances appropriate either to the CN-normal stars or to the solar ratio of C, N, and O. Thus, mixing into the O $\rightarrow$ N-process regions of the CN-strong stars must also be considered in order to conserve total C + N + O. The same conclusion was reached by BSH for their sample of SGB stars. Yet, O $\rightarrow$ N-processing occurs deeper within the star than does C $\rightarrow$ N and the convective mixing into C $\rightarrow$ N process regions of MS stars alone is difficult to explain in terms of the standard theory of stellar evolution. However, if the assumption of an initial solar CNO abundance ratio, or the assumption that CN-normal stars represent the original cluster abundance, is dropped, as has been suggested for other clusters, then the C + N = constant constraint may be met. This requires that both the CN-strong and the CN-normal stars be mixed to some extent.

There is apparently little difference in the range of C and N abundances among the MS stars compared to the SGB and cooler stars. This implies not only that the CN abundance altering mechanism responsible for the CN-bimodality is in operation as early as the MS, but that little change in the CN abundances occurs as the stars evolve further. A check of the latter would be a determination of the ratio of the number of CN-strong to CN-normal stars on the MS and a comparison of this value to similar ratios for the cooler, more evolved stars. It would be surprising if there were indeed no such mechanism, in view of the composition differences seen in objects as diverse as extreme Population I and II giants and the metal-poor cluster red giants.

Any scenario which attributes the CN variations to internal or mixing processes within individual stars must postulate that such processes have operated prior to the upper MS. Difficulties in modeling such processes, and the problems with the resulting evolutionary tracks are discussed in Da Costa & Demarque (1982) and VandenBerg & Smith (1988). The basic problem is that the early mixing of material into the CN-process region will supply fresh hydrogen fuel for energy generation causing at the least, a widening of the CM-diagram near the turnoff. An examination of Figure 1 shows that there is no such preferential distribution of the stars based on CN band strength (i.e., the CN-strong stars are not redder than the CN-normal ones). By analogy with the case of high O abundances, stars with primordially high N abundances should evolve at redder $B-V$ colors, although the relatively low abundance of

N compared to O, would mean that the redward shift is very small (VandenBerg 1985). Thus, the existence of stars with high primordial N abundances does not contradict the tightness of the CM-diagram in the turn off region as observed by Hesser et al. (1987).

There remain many possible explanations for the CN bimodal clusters that have been widely discussed in the literature. One is the idea that the stars formed out of material originally inhomogeneous in CN and CH, due to an earlier epoch of massive stars. This has the added advantage of possibly explaining the Na correlation with CN, as has also been observed in 47 Tuc and other CN-bimodal clusters. Another possibility, discussed by VandenBerg & Smith (1988), is the mixing of stars during the pre–ZAMS stage. However, the question of why globular cluster stars should undergo this form of mixing, and not field stars, remains unanswered (this would be necessary to explain the low numbers of CN-rich field dwarfs). Also, should this be the case, it will be relatively indistinguishable from a primordial variation, with the possible exception of very low $^{12}C/^{13}C$ ratios which should be found even in these faint stars. Such problems appear to require the new generation of large telescopes for the necessary observations.

The MgH and Mg *b* index, Mg_2 was also measured and compared to synthetic spectra with the result that while there is no Mg versus CN correlation in 47 Tuc, there appears to be a slight overall [Mg/A] excess.

We would like to thank G. H. Smith of the Lick Observatory for several important contributions to this work, especially in the discussions during the formative stages and contributions to the interpretations. We are grateful to S. Heathcote for expertly installing, and instructing us in the use of the 2D-FRUTTI system, and for allowing us to use the bulk of his engineering night for our program. We also thank N. Saavedra and P. Ugarte for assistance at the telescope, and Lisa Wells for help with IRAF in La Serena. We are also grateful to R. D. Cannon and R. A. Stathakis, whose preliminary reductions of the AAT fibre data provided invaluable guidance in the selection of objects which were observed. The spectrum synthesis calculations were assisted by J. Ohlmacher and made using the Cray Y-MP/864 of the San Diego Supercomputer Center. Part of this work was supported by the National Science Foundation under grant AST 89-18461.

REFERENCES

Bell, R. A., Briley, M. M., & Smith, G. H. 1990, AJ, 100, 187
Bell, R. A., Dickens, R. J., & Gustafsson, B. 1975, BAAS, 7, 535
Bell, R. A., & Gustafsson, B. 1978, A&AS, 34, 229
Bell, R. A., Hesser, J. E., & Cannon, R. D. 1983, ApJ, 269, 580
Briley, M. M., Bell, R. A., Hoban, S., & Dickens, R. J. 1990, ApJ, 359, 307
Briley, M. M., Bell, R. A., Smith, G. H., & Hesser, J. E. 1989, ApJ, 341, 800 (BBSH)
Brown, J. A., & Wallerstein, G. 1989, AJ, 98, 1643
Carbon, D. F., Barbuy, B., Kraft, R. P., Friel, E. D., & Suntzeff, N. B. 1987, PASP, 99, 335
Carbon, D. F., Langer, G. E., Butler, D., Kraft, R. P., Suntzeff, N. B., Kemper, E., Trefzger, C. F., & Romanishin, W. 1982, ApJS, 49, 207
Clegg, R. E. S., Lambert, D. L., & Tomkin, J. 1981, ApJ, 250, 262
Cottrell, P. L., & Da Costa, G. S. 1981, ApJ, 245, L79
Da Costa, G. S., & Demarque, P. 1982, ApJ, 259, 193
Dickens, R. J., Bell, R. A., & Gustafsson, B. 1979, ApJ, 232, 428
Faber, S. M., Friel, E. D., Burstein, D., & Gaskell, C. M. 1985, ApJS, 57, 711
Genova, F., & Schatzman, E. 1979, A&A, 78, 323
Gustafsson, B., Bell, R. A., Eriksson, K., & Nordlund, Å. 1975, A&A, 42, 407
Hesser, J. E. 1978, ApJ, 223, L117
Hesser, J. E., & Bell, R. A. 1980, ApJ, 238, L149
Hesser, J. E., Harris, W. E., VandenBerg, D. A., Allwright, J. W. B., Shott, P., & Stetson, P. 1987, PASP, 98, 739
Hesser, J. E., and Hartwick, F. D. A. 1977, ApJS, 33, 361
Hesser, J. E., Hartwick, F. D. A., & McClure, R. D. 1976, ApJ, 207, L113
———. 1977, ApJS, 33, 471
Hesser, J. E., Shawl, S. J., & Meyer, J. E. 1986, PASP, 98, 403
Kjaergaard, P., Gustafsson, B., Walker, A. G. H., & Hultqvist, L. 1982, A&A, 115, 145
Laird, J. B. 1985, ApJ, 289, 556
Lambert, D. L., & Ries, L. M. 1981, ApJ, 248, 228
Langer, G. E., Kraft, R. P., and Friel, E. D. 1985, PASP, 97, 373
Lee, S. W. 1977, A&AS, 27, 381
Lloyd Evans, T., Menzies, J. W., & Smith, G. H. 1982, MNRAS, 201, 137
Mallia, E. A. 1978, A&A, 70, 115
Mayor, M., Imbert, M., Anderson, J., Ardeberg, A., Benz, W., Lindren, H., Martin, N., Maurico, E., Nordström, B., & Prévot, L. 1984, A&A, 134, 118
Norris, J. 1978, IAU Symposium 80, The HR Diagram, ed. A. G. Davis Philip & D. S. Hayes (Dordrecht: Reidel), p. 195
———. 1987, ApJ, 313, L65
Norris, J., & Cottrell, P. L. 1979, ApJ, 229, L69
Norris, J., Cottrell, P. L., Freeman, K. C., & Da Costa, G. S. 1981, ApJ, 244, 205
Norris, J., & Freeman, K. C. 1979, ApJ, 230, L179
———. 1982, ApJ, 254, 143
Norris, J., Freeman, K. C., & Da Costa, G. S. 1984, ApJ., 277, 615
Proffitt, C., & Michaud, G. 1990, in Cool Stars, Stellar Systems, and the Sun, ed. G. Wallerstein (ASP Conf. Ser., 9), in press
Smith, G. H. 1987, PASP, 99, 67
Smith, G. H., & Bell, R. A. 1986, AJ, 91, 1121
Smith, G. H., Bell, R. A., & Hesser, J. E. 1989, ApJ, 341, 190 (SBH)
Smith, V. V., & Suntzeff, N. B. 1990, preprint
Spite, F., & Spite, M. 1986, A&A, 163, 140
Suntzeff, N. B. 1981, ApJS, 47, 1
———. 1988, in IAU Gen. Assembly No. 20, The Abundances of Stars within Globular Clusters: Spectroscopy of Individual Stars, ed. G. Cayrel de Strobel, M. Spite, & T. Loyd Evans (Paris: Paris Observatory), p. 71
Tomkin, J., & Lambert, D. L. 1984, ApJ, 279, 220
Trefzger, C. F., Carbon, D. F., Langer, G. E., Suntzeff, N. B., & Kraft, R. P. 1983, ApJ., 266, 144
VandenBerg, D. A. 1985, in Production and Distribution of C, N, and O Elements, ed. I. J. Danziger, F. Matteucci, & K. Kjär (Garching bei München: ESO), p. 73.
VandenBerg, D. A., & Smith, G. H. 1988, PASP, 100, 314
Wheeler, J. C., Sneden, C., and Truran, J. W., Jr. 1989, ARAA, 27, 279